

Supplementary Information

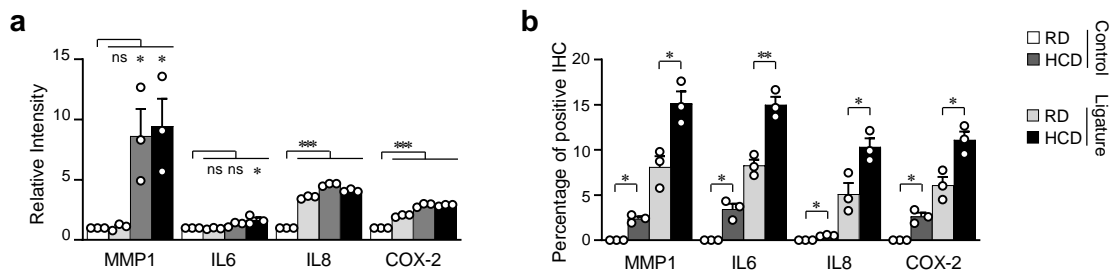
Disruption of cholesterol homeostasis triggers periodontal inflammation and alveolar bone loss

Thanh-Tam Tran^{1,2}, Gyuseok Lee^{1,2}, Yun Hyun Huh³, Ki-Ho Chung⁴, Sun Young Lee¹, Ka Hyon Park¹, Seung Hee Kwon², Min-Suk Kook⁵, Jang-Soo Chun³, Jeong-Tae Koh^{1,2}, Je-Hwang Ryu^{1,2*}

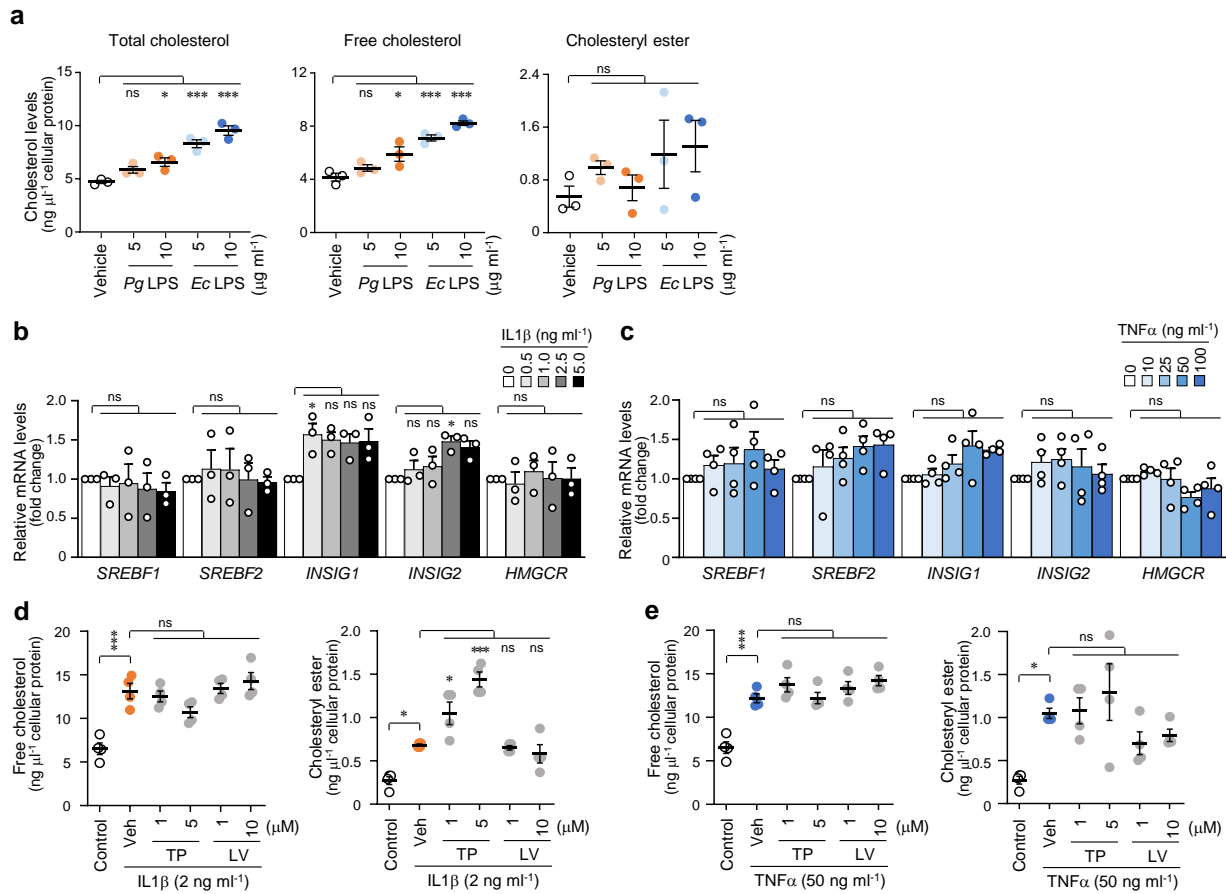
Supplementary Figure 1 to 7

Supplementary Table

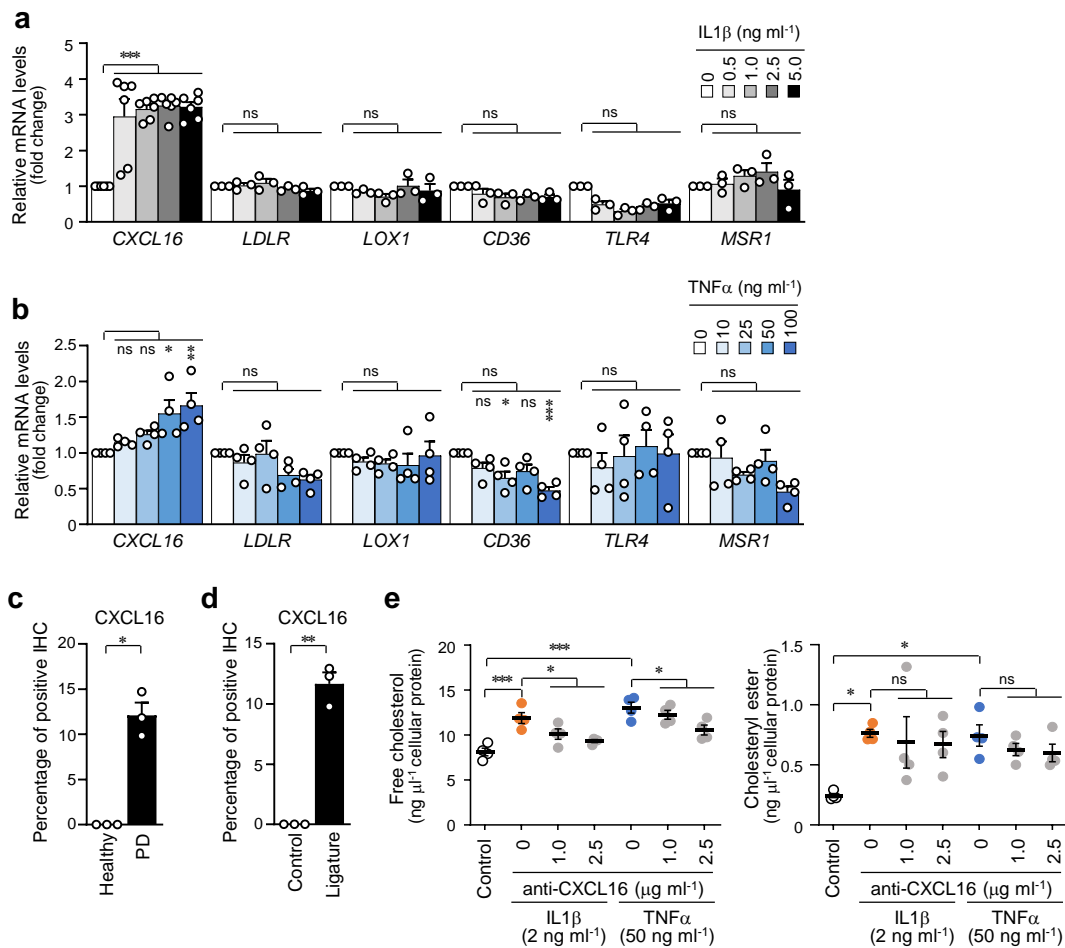
Supplementary Figures



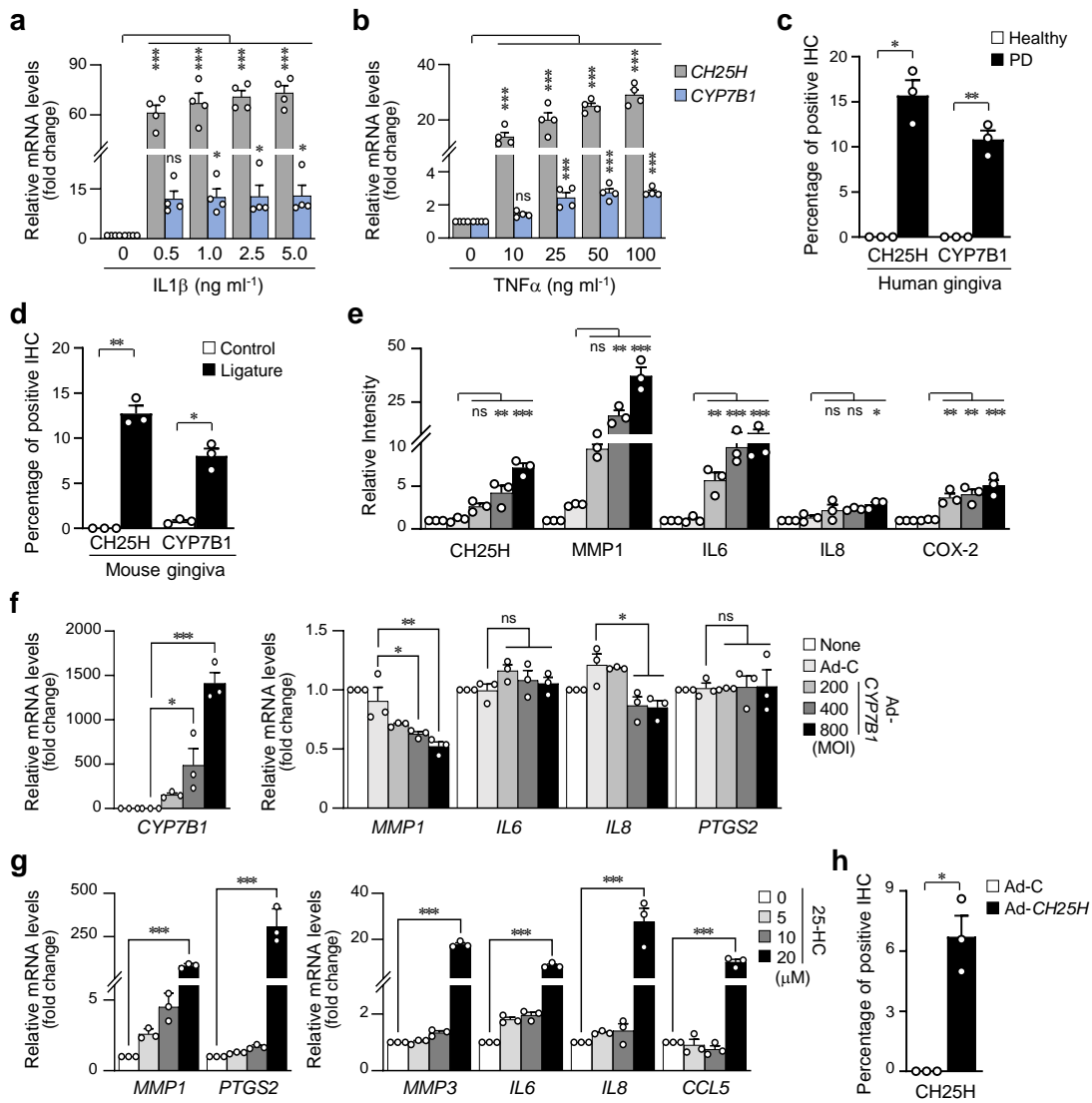
Supplementary Fig. 1. Quantification of western blot and immunohistochemistry staining results. **a** Relative intensity of the indicated proteins in human GF treated with cholesterol for 36 h ($n = 3$). **b** Percentage of positive staining for MMP1, IL6, IL8, and COX-2 immunostaining in images from ligature-induced PD mice fed with RD or HCD ($n = 3$). Values are presented as mean \pm SEM via two-tailed *t*-test (**b**) and one-way ANOVA with Tukey's test (**a**). (* $P < 0.05$, ** $P < 0.01$, *** $P < 0.001$).



Supplementary Fig. 2. Expression of cholesterol biosynthesis-related genes and effects of cholesterol biosynthesis inhibitors. **a** Total cholesterol, free cholesterol, and cholesteryl ester levels in human GF treated with *Pg* LPS or *Ec* LPS for 24 h ($n = 3$). **b, c** qRT-PCR analysis of the indicated genes involved in cholesterol sensing and synthesis in human GF treated with IL1 β (**b**) ($n = 3$) or TNF α (**c**) ($n = 4$) for 24 h. **d, e** Cellular levels of free cholesterol and cholesteryl ester in human GF treated with cholesterol synthesis inhibitors (triparanol [TP] and lovastatin [LV]) in the presence of IL1 β (2 ng ml^{-1}) (**d**) or TNF α (50 ng ml^{-1}) (**e**) for 24 h ($n = 4$). n indicates the number of biologically independent samples. Values are presented as mean \pm SEM with one-way ANOVA and Tukey's test. (* $P < 0.05$, ** $P < 0.01$, *** $P < 0.001$).

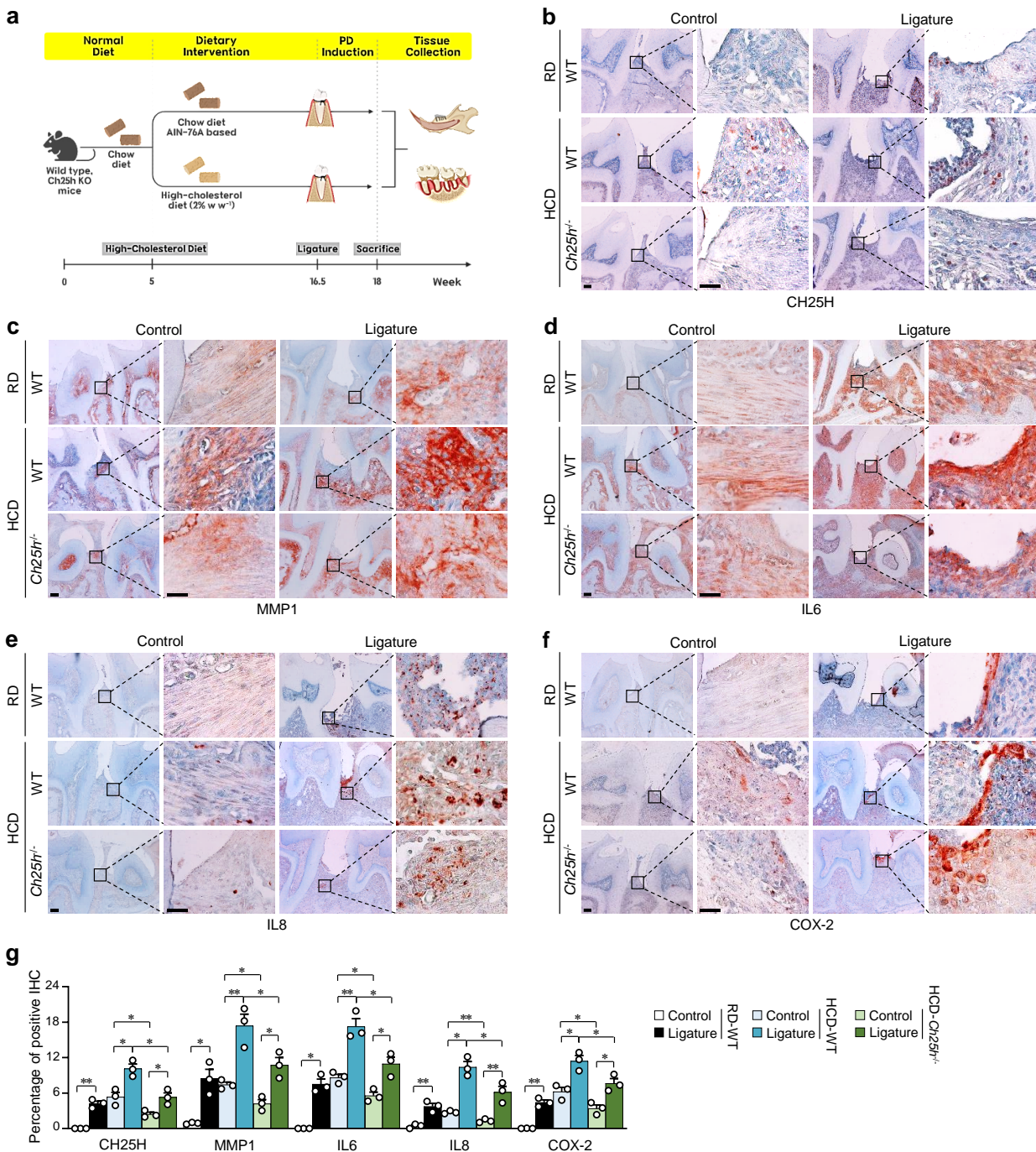


Supplemental Fig. 3. Upregulation of CXCL16 in inflamed periodontal cells and tissues and CXCL16-mediated increase in cellular cholesterol in GF. **a, b** Evaluation of mRNA levels of genes involved in cholesterol uptake in human GF treated with IL1 β (**a**) or TNF α (**b**) for 24 h ($n \geq 3$). **c, d** Percentage of positive staining intensity of CXCL16 immunostaining of the gingiva from human patients with PD (**c**) and ligature-induced PD mice (**d**) ($n = 3$). **e** Cellular levels of free cholesterol and cholestryl ester in human GF treated with anti-CXCL16 blocking antibody in the presence of IL1 β (2 ng ml $^{-1}$) or TNF α (50 ng ml $^{-1}$) for 24 h ($n = 4$). n indicates the number of biologically independent samples. Values are presented as mean \pm SEM via two-tailed t -test (**c, d**) and one-way ANOVA and Tukey's test (**a, b, e**). (* $P < 0.05$, ** $P < 0.01$, *** $P < 0.001$).



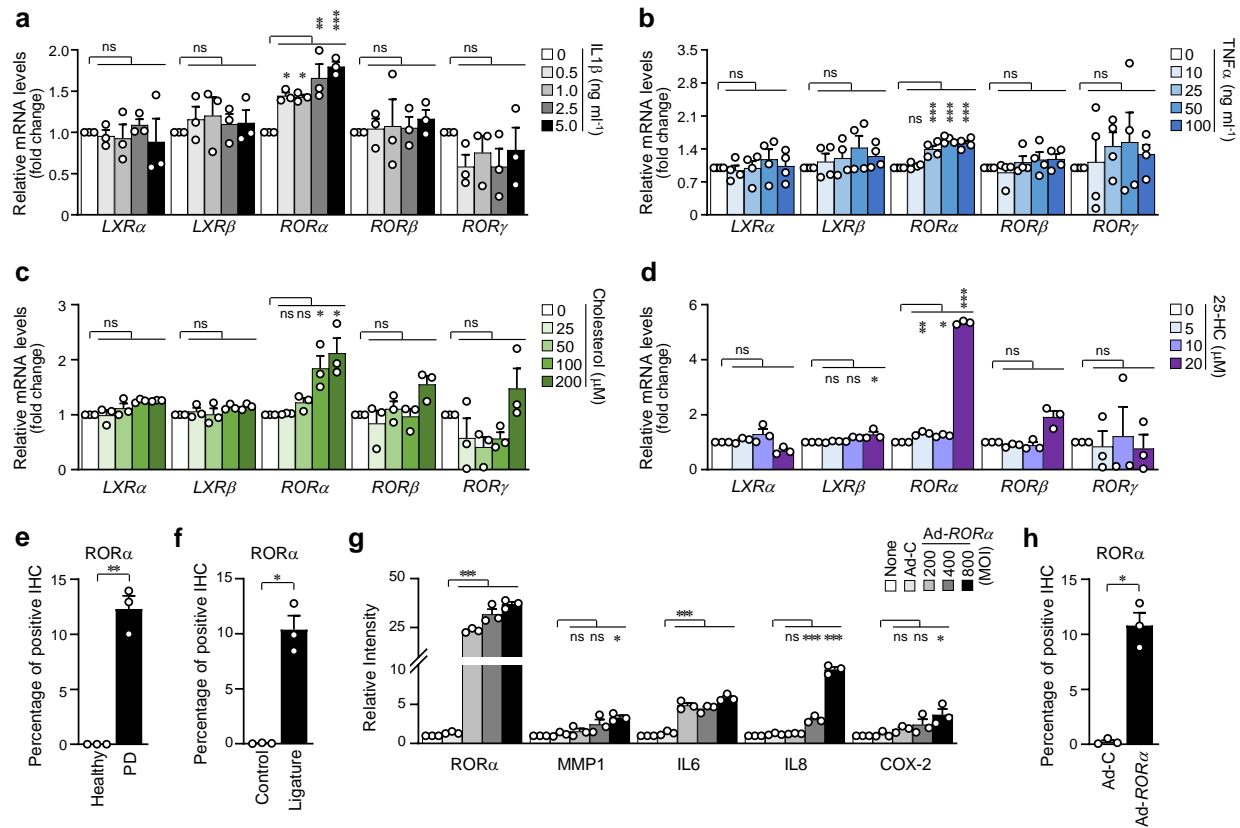
Supplementary Fig. 4. Upregulation of CH25H and CYP7B1 in PD-mimicking conditions and their functions in PD-associated catabolic gene expression. **a, b** mRNA levels of *CH25H* and *CYP7B1* in human GF treated with the indicated doses of IL1 β or TNF α for 24 h ($n = 4$). **c, d** Graphical representation of percentage of positive staining intensity of CH25H and CYP7B1 immunostaining images in human (**c**) and mouse gingiva (**d**) ($n = 3$). **e** Relative intensities of CH25H, MMP1, IL6, IL8, and PTGS2 western blot images of human GF infected with *CH25H*-overexpressing adenovirus (Ad-*CH25H*; $n = 3$). **f** mRNA levels of *CYP7B1*, *MMP1*, *IL6*, *IL8*, and **g** mRNA levels of *MMP1*, *PTGS2*, *MMP3*, *IL6*, *IL8*, and *CCL5* in Ad-*CH25H* infected cells. **h** Positive IHC staining in Ad-*CH25H* infected cells.

PTGS2 in human GF infected with Ad-*CYP7B1* ($n = 3$). **g** mRNA levels in human GF treated with 25-HC for 48 h ($n = 3$). **h** Percentage of positive staining intensity of CH25H immunostaining images of mouse gingiva injected with an empty virus (Ad-C) or Ad-*Ch25h* (1×10^9 PFU per 5 μ l) ($n = 3$). n indicates the number of biologically independent samples. Values are presented as mean \pm SEM based on two-tailed *t*-test (**c, d, h**) and one way ANOVA and Tukey's test (**a, e, f, g**). (* $P < 0.05$, ** $P < 0.01$, *** $P < 0.001$).

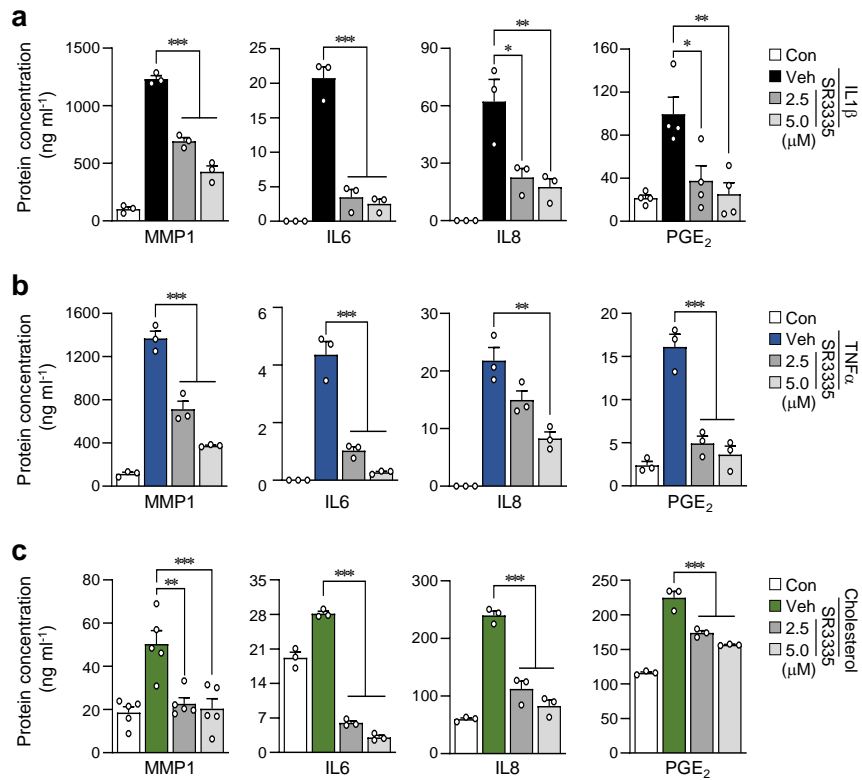


Supplementary Fig. 5. Alterations in PD-associated protein expression in *Ch25h*^{-/-} mice. **a** Schematic diagram of experimental ligature-induced PD procedures of mice fed with RD or HCD for 13 weeks. Schematic diagram was created with BioRender.com. **b-f** Representative images of CH25H (**b**), MMP1 (**c**), IL6 (**d**), IL8 (**e**), and COX-2 (**f**) immunostaining from control and ligature-

induced PD gingiva of wild-type (WT) and *Ch25h* knockout (*Ch25h*^{-/-}) mice fed RD or HCD for 13 weeks. Scale bar, 100 μm (left), 25 μm (right). **g** Graphical representation of percentage of positive staining intensity of CH25H, MMP1, IL6, IL8, and COX-2 immunostaining images from control and ligature induced PD gingiva of wild-type (WT) and *Ch25h* knockout (*Ch25h*^{-/-}) mice fed RD or HCD for 13 weeks ($n = 3$). Values are presented as mean \pm SEM based on two-tailed *t*-test (**g**). (* $P < 0.05$, ** $P < 0.01$, *** $P < 0.001$).



Supplementary Fig. 6. ROR α expression is upregulated in PD-mimicking human GF. **a-d** qRT-PCR analysis of mRNA levels of nuclear receptors (*LXR α* , *LXR β* , *ROR α* , *ROR β* , *ROR γ*) in human GF treated with the indicated doses of IL1 β (**a**), TNF α (**b**), cholesterol (**c**), or 25-HC (**d**) for 24 h ($n \geq 3$). **e, f** Percentage of positive staining for *ROR α* immunostaining in images from human (**e**) and mouse gingiva (**f**) ($n = 3$). **g** Relative intensities of *ROR α* , MMP1, IL6, IL8, and PTGS2 western blot images in human GF infected with Ad-*ROR α* for 48 h ($n = 3$). **h** Percentage of positive staining intensity of *ROR α* immunostaining images in mouse gingiva injected with an empty virus (Ad-C) or Ad-*Rora* (1×10^9 PFU per 8 μ l) ($n = 3$). n indicates the number of biologically independent samples. Values are presented as mean \pm SEM based on two-tailed *t*-test (**e, f, h**) and one-way ANOVA and Tukey's test (**a, b, c, d, g**). (* $P < 0.05$, ** $P < 0.01$, *** $P < 0.001$).



Supplemental Fig. 7. Blocking of ROR α activation reduced the effects of IL1 β , TNF α , and cholesterol on the expression of catabolic factors. **a-c** Secretion of MMP1, IL6, and IL8 and production of PGE₂ from human GF treated with the indicated concentrations of SR3335 in the presence of IL1 β (2 ng ml⁻¹) (**a**), TNF α (50 ng ml⁻¹) (**b**), and cholesterol (200 μ M) (**c**) for 24 h ($n \geq 3$). n indicates the number of biologically independent samples. Values are presented as mean \pm SEM based on one-way ANOVA and Tukey's test. (* $P < 0.05$, ** $P < 0.01$, *** $P < 0.001$).

Supplementary Table. PCR primer sequence and PCR condition

Gene	Strand	Primer sequences	Size (bp)	AT (°C)	Origin
<i>CCL5</i>	S	5'-GGATCAAGACAGCACGTGGA-3'	421	60	Human
	AS	5'-CGGGTGGGGTAGGATAGTGA-3'			
<i>CD36</i>	S	5'-GAGAACTGTTATGGGGCTAT-3'	389	60	Human
	AS	5'-TTCAACTGGAGAGGCAAAGG-3'			
<i>CH25H</i>	S	5'-ACATCTGGCTTCCGTGGAG-3'	139	60	Human
	AS	5'-TACGGAGCGAACAGTTGCAGTT-3'			
<i>CYP7B1</i>	S	5'-TGCTGCAGTCAACAGGTCAA-3'	193	60	Human
	AS	5'-TTTCGCCACACAGTAGTCCCC-3'			
<i>CXCL16</i>	S	5'-ATCTGCTTTCACACTGGGT-3'	485	60	Human
	AS	5'-GAGGGGAAACCATCAGCAAA-3'			
<i>GAPDH</i>	S	5'-GGTGAAGGTCGGAGTCAACG-3'	327	60	Human
	AS	5'-CAAATGAGCCCCAGCCTTCT-3'			
<i>HMGCR</i>	S	5'-TTGGTGTGGAGCTTGTGT-3'	267	60	Human
	AS	5'-CGAGCCAGGCTTCACTTCT-3'			
<i>IL6</i>	S	5'-AGGCTGGACTGCAGGAACCTCTAAAG-3'	421	60	Human
	AS	5'-CCCTGAGAAAGGAGACATGTAACAAGAG-3'			
<i>IL8</i>	S	5'-CTCTCTGGCAGCCTCCTGATTTC-3'	254	60	Human
	AS	5'-AAACTCTCCACAACCCTCTGCAC-3'			
<i>INSIG1</i>	S	5'-CATCTTCTCCCGCCTGGT-3'	247	60	Human
	AS	5'-ATGTCCACCAAAGGCCAAA-3'			
<i>INSIG2</i>	S	5'-GCGGGGGATTCTGGTAGG-3'	476	60	Human
	AS	5'-ACACCGCATTACACTGGACC-3'			
<i>LDLR</i>	S	5'-TGTTCCCACGTCTGCAATGA-3'	298	60	Human
	AS	5'-GGATGAGGCTGGTACTCG-3'			
<i>LOX1</i>	S	5'-GGCATGCAATTATCCCAGGTG-3'	283	60	Human
	AS	5'-TGCCAGATCCAGTCTTGC-3'			
<i>LXRα</i>	S	5'-ACTGATGTTCCCACGGATGC-3'	338	60	Human
	AS	5'-CACAGTGTAGCGAGGGCT-3'			
<i>LXRβ</i>	S	5'-CACAGTCACAGTCGCAGTCA-3'	208	60	Human
	AS	5'-TCGGAGAAGGAGCGTTGTT-3'			
<i>MMP1</i>	S	5'-GGAGGGGATGCTCATTGATG-3'	541	60	Human
	AS	5'-TAGGAAAGCCAAGGAGCTGT-3'			

<i>MMP3</i>	S	5'-AATCCTACTGTTGCTGTGCGTG-3'	238	60	Human
	AS	5'-CAGAGTGTGGAGTCCAGCTTC-3'			
<i>MSR1</i>	S	5'-CCAATGAGAGGGATGAGAACTG-3'	129	60	Human
	AS	5'-GCTCAATGACAGCTTGCTTC-3'			
<i>PTGS2</i>	S	5'-AATCCTTGCTGTTCCCACCCATG-3'	329	60	Human
	AS	5'-AAGGGAGTCGGGCAATCATCAGG-3'			
<i>RORα</i>	S	5'-GCAGATAACGTGGCAGACCT-3'	412	60	Human
	AS	5'-GCGATCCGCTGACATCAGTA-3'			
<i>RORβ</i>	S	5'-GGGTTATTACAACGTCGATTCCG-3'	358	60	Human
	AS	5'-CGTATTGGATGGCGTGAGTG-3'			
<i>RORγ</i>	S	5'-GCTCTGGGCCCTCATATTG-3'	315	60	Human
	AS	5'-TGGCATGTCTCCCTGTAGG-3'			
<i>SREBF1</i>	S	5'-CTGTTGGTGCTCGTCTCCTT-3'	214	60	Human
	AS	5'-CTACAAGCCAGGTCCAGGTG-3'			
<i>SREBF2</i>	S	5'-CAACT CCT ATT CTT CAGCCCCG-3'	460	60	Human
	AS	5'-CGTCTGGATAGGGGTGGTGA-3'			
<i>TLR4</i>	S	5'-AACCTCCCCTCTAACCAA-3'	496	60	Human
	AS	5'-TCATAGGGTTCAGGGACAGGT-3'			

AT, annealing temperature; S, sense; AS, antisense.